Effects of interelectrode impedance in water conductivity measurements with capacitive electrodes

Carles Aliau-Bonet
Instrumentation, Sensors and Interfaces Group
Universitat Politècnica de Catalunya, BarcelonaTech (UPC)
Castelldefels, Spain
carles.aliau@upc.edu

Ramon Pallas-Areny
Instrumentation, Sensors and Interfaces Group
Universitat Politècnica de Catalunya, BarcelonaTech (UPC)
Castelldefels, Spain
ramon.pallas@upc.edu

***Abstract*—Capacitive electrodes overcome electrode polarization problems and enable noninvasive measurements hence they do not obstruct flow and avoid corrosion, wearing and soiling. However, their impedance is much higher than that of direct contact electrodes and, to reduce it, the measurement frequency must be increased, which worsens the effects of stray interelectrode impedance. In this paper, we analyse those effects when measuring water conductivity inside a plastic container and determine the more convenient frequency range to minimise measurement deviations.**

***Keywords*—water conductivity; capacitive electrodes; interelectrode capacitance; interelectrode resistance; shielding.**

I. Introduction

Water conductivity can be measured with capacitive electrodes, also termed contactless electrodes [1] [2], which do not stablish any electrical contact between electrode and water. There is only a mechanical contact, usually with the container. This avoids electrochemical reactions [1] and, for non-immersed electrodes, electrodes do not deteriorate because of abrasion or soiling, neither do they obstruct flow.

The electrode-water interface in capacitive electrodes comprises a conductor (electrode), a dielectric and water. The interfacial double layer between the dielectric and water is very thin hence its capacitance is much larger than that between the conductor and the dielectric-water interface. As a result, the equivalent capacitance of the electrode-water interface is that determined by electrode area and dielectric thickness, and will seldom exceed about 50 pF for electrodes of some square centimetres [3]. Then, for the current through the sample to be measurable, electrode impedance must be reduced, which asks for high-frequency excitation. However, this also reduces interelectrode impedance, that is, the impedance between electrodes in the absence of the sample. In this paper we analyse the effect of this stray impedance and determine the suitable frequency range for the measurements to be valid.

II. Impedance Model

Fig. 1 shows the model of the whole impedance measured. R_x is water resistance, which depends on water conductivity σ and the cell constant. R_x is shunted by C_x, which depends on water's electrical permittivity, ε. The characteristic frequency of water is $\omega_c = (R_x C_x)^{-1} = \sigma/\varepsilon$ [2]. Electrode impedance is modelled by capacitance C_e, which depends on the electrical permittivity of the insulating material of the water receptacle (plastic, ceramic, glass), shunted by R_e, which describes (dc) leakage currents in the dielectric. Since the resistivity of good insulators ranges from 1 TΩ × cm to 10 PΩ × cm [4], R_e will be very high. Finally, between any two conductors that can see each other, such as the electrodes in the cell, there is always some capacitance and, if they share a physical support, some leakage resistance, which will be very high if that support is an insulator. These are modelled by C_{hl} and R_{hl} in Fig 1.

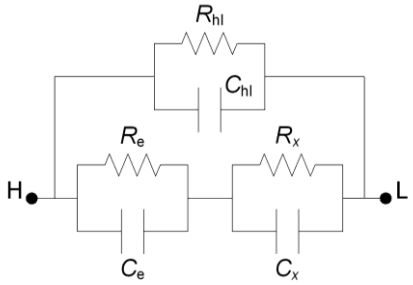

Fig. 1. Lumped-parameter model for bipolar impedance measurements.

Since C_e will not exceed about 50 pF, for water less pure than demineralized water ($\sigma < 5 \times 10^{-3}$ dS/m), below 100 kHz we will have $1/\omega C_e >> R_x$. In that case, the real part of the impedance between H and L can be approximated by

$$\mathrm{Re}\, Z_{HL} \approx \frac{R_x}{\left(1+C_{hl}/C_e\right)^2} \frac{1+\left(\omega_n/\omega\right)^2}{1+\left(\omega/\omega_d\right)^2} \tag{1}$$

where

$$\omega_n^{-2} = R_x \left(R_e \| R_{hl}\right) C_e^2 \tag{2}$$

and

$$\omega_d^{-1} = R_x \left(C_x + \frac{C_{hl} C_e}{C_{hl} + C_e} \right). \tag{3}$$

If $\omega_h << \omega_d$, which will normally be the case because R_x is much smaller than R_e and R_{hl}, and C_x and C_{hl} are smaller than C_e, from (1) we deduce that Re Z_{HL} is constant in the frequency band between ω_h and ω_d, and its value is $R_x/(1 + C_{hl}/C_e)$.

Equation (2) shows that Re Z_{HL} measurements below ω_h are hindered by electrode resistance, and that R_{hl} effectively shunts

R_e hence dc leakage between electrodes is equivalent to reduced electrode-water insulation.

Equation (3) means that Re Z_{HL} starts to decrease for increasing frequencies close to ω_h, whereas if C_{hl} were zero it would not decrease until frequencies close to ω_c, which is higher than ω_h. That is, large C_{hl} and low water conductivity narrow the frequency band where Re Z_{HL} is constant.

The imaginary part of the impedance between H and L is

$$\mathrm{Im}\, Z_{HL} \approx \frac{-1}{\omega(C_{hl}+C)} \qquad (4)$$

where $C_{hl} + C$ is the equivalent series capacitance C_s between H and L. For frequencies well below ω_h, C equals C_e, whereas for frequencies well above ω_h, C equals $C_eC_x/(C_e+C_x)$. Therefore, if C_e is known, the correction factor required to obtain R_x from (1) could be obtained by measuring Im Z_{HL}, for example, at the same frequency than Re Z_{HL}.

III. Materials and Methods

We have measured Re Z_{HL} and Im Z_{HL} for two different water samples inside a cell built from a 12 cm-long 100 mL polypropylene syringe Omnifix® (B. Braun Melsungen AG), which respective external and internal diameters were 30.6 mm and 28.0 mm. The capacitive electrodes were two 25 mm-wide copper strips wrapped around the syringe and whose inner ends were 50 mm apart. Their equivalent capacitance C_e was estimated to be about 17.4 pF ± 0.1 pF by measuring C_s at low frequency (10 kHz) with a battery-supplied capacitance meter (Agilent U1733C), when the water sample conductivity was 1 dS/m. The cell was connected to an impedance analyser (Agilent 4294A) by two 90 mm-long cables with 1 mm^2 cross section. To fix the electromagnetic environment and avoid external capacitive couplings, the syringe was placed inside a 30 cm-long oval cylinder (17 cm and 15 cm in diameter) built by folding a steel wire mesh, with 7 mm wire spacing, as shown in Fig.2. The mesh was connected to terminal H, thus ensuring that no electric field lines emanating from the H terminal would end outside the mesh. Two positions of the cell were tested: first, when resting on the base of the cylindrical shield (position #1), and second when placed along its longitudinal axis (position #2).

The frequency range of interest was 1 kHz-10 MHz. The electrical conductivity of the two water samples used, measured with a Tetracon® 325 probe connected to a WTW conductivity meter model 340i, were 0.01 dS/m (10 ± 1 µS/cm) and 1 dS/m (1000 ± 6 µS/cm), referred to 25.0 °C. Since the samples were at 16.0 °C, the corrected conductivities and permittivity were 8.2×10^{-3} dS/m, 0.82 dS/m and relative permittivity 81.6 [5]. Therefore, the characteristic frequencies of the samples were 181 kHz and 18.1 MHz, respectively.

IV. Experimental Results and Discussion

Fig. 3 shows Re Z_{HL} for 0.01 dS/m water. Solid lines are for position #1 (grey) and position #2 (black), at ambient conditions, and the broken grey line is for position #2 when a burst of moist air was blown onto the cell through the mesh.

The effect of ω_h is apparent below 1 kHz. The impedance of electrode capacitance at that frequency becomes comparable to electrode resistance shunted by the resistance of the external cell surface. From Table I, for position #1 (solid grey line), Re Z_{HL} at 1 kHz is 1.33 times that at 10 kHz, and for position #2 (solid black line) it is 1.21 hence very close as the two lines look almost parallel up to frequencies below 100 kHz. (Noisy curves at 1 kHz are due to the limited ability of the instrument to distinguish Re Z_{HL} from the much larger Im Z_{HL} at low frequencies.) The separation between the two solid curves is due to the factor $(1 + C_{hl}/C_e)^2$ in (1) because C_{hl} is larger when the cell is closer to the shield (position #1). From Table I, at 10 kHz the ratio between Re Z_{HL} for position #2 and position #1 is 1.52. This means that if for position #2 C_{hl}/C_e equals, for example, 0.1, then for position #1 it is 3.5 times larger.

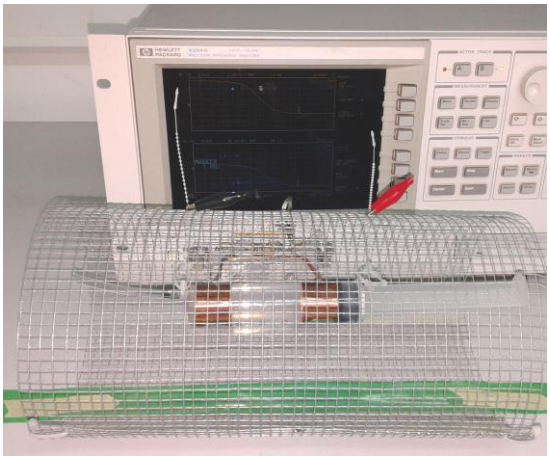

Fig. 2. Measurement cell surrounded by an electric shield.

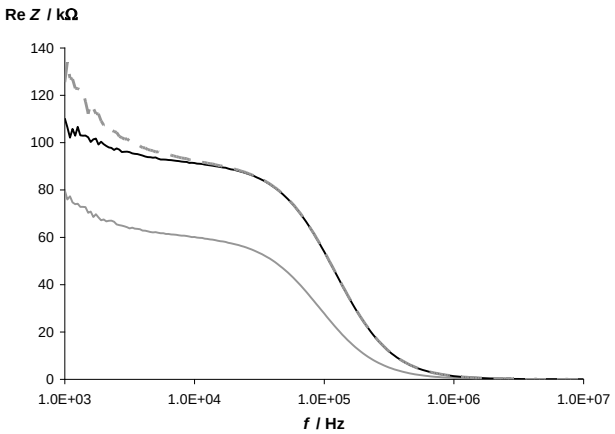

Fig. 3. Real part of Z_{HL} for 0.01 dS/m water and two different positions of the cell inside the cylindrical shield in ambient conditions (solid line), and when blowing hot air onto the cell in the second position (broken line).

Table I. Re Z_{HL} (kΩ) for 0.01 dS/m water.

f (kHz)	Position #1	Position #2, dry	Position #2, moist
1	79.9	110.3	125.5
10	60.1	91.4	92.5

When the measurement frequency in Fig. 3 approaches 100 kHz, the three curves decrease because of ω_d. At ω_d, Re Z_{HL} becomes half that in the flat zone, say at 10 kHz. Therefore, f_d is about 91 kHz when the cell is in position #1 and 120 kHz in position #2. For 0.01 dS/m water at 16 ºC, f_c is about 181 kHz. Therefore, Fig. 3 confirms that ω_d depends on C_{hl}: when C_{hl} decreases (position #2), f_d approaches f_c.

The broken line in Fig. 3 shows that when the external surface of the cell becomes moist, Re Z_{HL} increases. This is because R_{hl} decreases and, according to (2), ω_h increases hence from (1), Re Z_{HL} increases too: from 110.3 kΩ to 125.5 kΩ at 1 kHz, and from 91.4 kΩ to 92.5 kΩ at 10 kHz (Table I). At 25 kHz, the increase is negligible because 25 kHz is much higher than f_n. ω_d, however, stays the same for the moist surface because it does not depend on R_{hl}.

Fig. 4 shows the equivalent series capacitance C_s between H and L for 0.01 dS/m water. Since C_e is 17.4 pF and R_x is about 100 kΩ, at 1 kHz $1/\omega C_e$ is about 9 MΩ and the condition $1/\omega C_e >> R_x$ for (1) to be valid, is fulfilled. Therefore, given that at low frequencies we have $C_s \approx C_{hl} + C_e$ and C_e is constant, the decrease in C_s from position #1 to position #2 at 1 kHz is probably due to the decrease in C_{hl} when the cell is moved from the bottom to the centre of the shield. For C_e = 17.4 pF, from Table II we obtain $C_{hl} \approx 8$ pF for position #1 and $C_{hl} \approx 3.3$ pF for position #2. Therefore, the ratio between the factor $(1 + C_{hl}/C_e)^2$ in (1) for the two positions is 1.50 hence very close to the 1.52 ratio obtained from Fig. 3. Blowing onto the cell increases C_s by 0.2 pF as water vapour condensates on the external cell surface, which was at 16.0 °C.

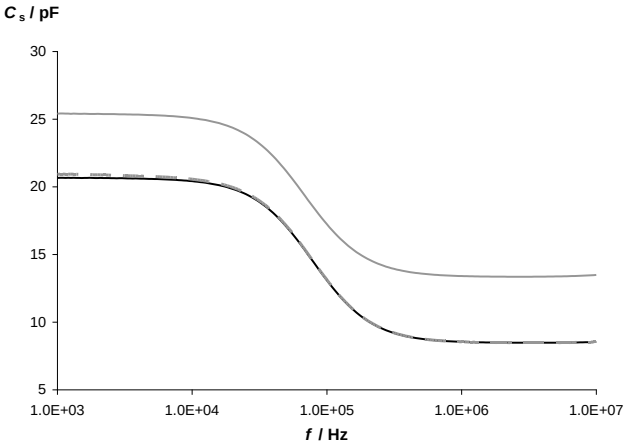

Fig. 4. Equivalent series capacitance for 0.01 dS/m water.

TABLE II. C_S (pF) FOR 0.01 dS/m WATER.

f (kHz)	Position #1	Position #2, dry	Position #2, moist
1	25.4	20.7	20.9
10	25.1	20.4	20.6

The separation between C_s values at 10 MHz should also be 4.7 pF, because C_e and C_x do not depend on the position of the cell, yet that difference is 4.9 pF in Fig. 4. This may be due to wave propagation effects because at 10 MHz we have $\lambda/126$ = 2.6 cm hence smaller than electrode separation yet it should be much smaller to avoid propagation effects [6].

For 1 dS/m water, Fig. 5 shows that C_s is constant up to about 1 MHz and then it starts to decrease, instead of displaying two flat zones ("low frequency" and "high frequency") separated by a transition zone, as in Fig. 4. Table III confirms that C_s remains almost constant with frequency from 1 kHz to 1 MHz. This is because the characteristic frequency is directly proportional to conductivity hence f_c is also 100 times larger now. Consequently, the "low frequency" zone extends up to two more frequency decades, which explains why C_s values at 1 MHz in Table III are close to those at 10 kHz in Table II. Blowing air onto the cell increases C_s again, as shown in the right-most column in Table III.

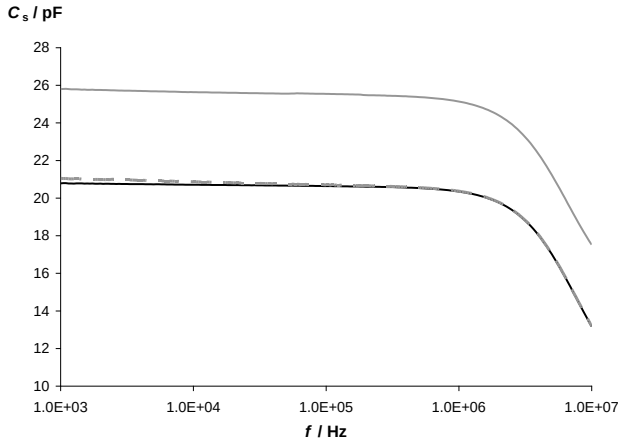

Fig. 5. Equivalent series capacitance for 1 dS/m water.

TABLE III. C_S (pF) FOR 1 dS/m WATER.

f (kHz)	Position #1	Position #2, dry	Position #2, moist
1	25.8	20.8	21.0
10	25.6	20.7	20.9
100	25.5	20.6	20.7
1000	25.1	20.3	20.4

Fig. 6 shows the real part of Z_{HL} for 1 dS/m water when the cell is centred inside the shield. The solid line is for the "dry" cell (at ambient conditions), whereas the broken line was obtained after blowing onto the cell. The effect of ω_d does not become apparent until approaching 10 MHz, as expected, because for 0.01 dS/m water, 100 times less conductive, hence R_x 100 times higher, it was visible below 100 kHz (Fig. 3). R_x decrease also affects ω_h, which increases by the same factor.

Table IV shows how the fast increase of Re Z_{HL} below 1 MHz would result in gross errors as its value, with respect to that at 1 MHz, is 1.19 times higher at 100 kHz, 2.98 times higher at 10 kHz and 26.5 times higher at 1 kHz. When R_x decreases, Re Z_{HL} increases because of the higher ω_h, as predicted by (1). This is relevant because if the electrodes were assumed to be ideal (infinite insulation), and interelectrode impedance was neglected, it would be assumed Re $Z_{HL} = R_x$, and the major measurement constraint would be the

disproportion between R_x and the much larger electrode impedance at low frequencies with respect to ω_t. But, in practice, the measurement frequency must be relatively high for the real part of the equivalent electrode impedance to be much smaller than the (small) R_x. Then, even at that "high" frequency there is still a measurement deviation due to C_{hl}/C_e.

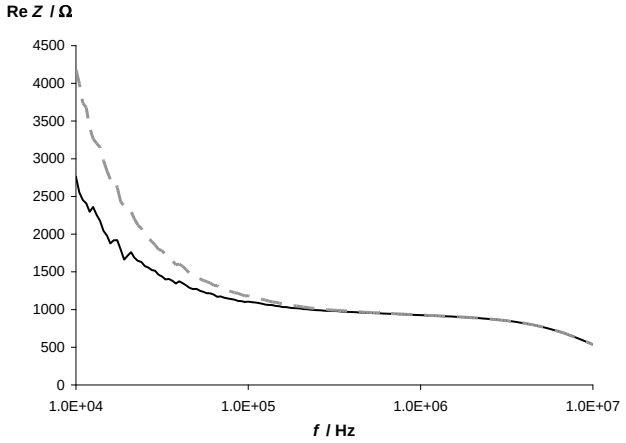

Fig. 6. Real part of Z_{HL} for 1 dS/m water with the cell centred inside the cylindrical shield in ambient conditions (solid line), and when blowing hot air onto the cell in the second position (broken line).

TABLE IV. RE Z_{HL} (Ω) FOR 1 dS/m WATER.

f (kHz)	Position #1	Position #2, dry	Position #2, moist
1	-	24552	43525
10	-	2763	4183
100	796	1105	1183
1000	605	926	928

The effect of $(1+ C_{hl}/C_e)^2$ in (1) can be checked again by dividing Re Z_{HL} at 1 MHz in column 3 of Table IV by the corresponding value in column 2. The result is 1.53, which is very close to the value obtained for 0.01 dS/m water in Table I (1.52). This means that C_{hl} depends only on the position of the cell, not on water conductivity.

Water condensation on the external surface of the cell increases Re Z_{HL} again: from 1105 Ω to 1183 Ω at 100 kHz, 7 % larger, and from 24552 Ω to 43525 Ω at 1 kHz, 77 % larger.

During measurements, hands or body movements near the cell did not affect the results thus corroborating the efficacy of the shield. However, shield closeness to electrodes increased C_{hl}, which in the absence of the shield would be below 1 pF. The large C_{hl} values relative to C_e allowed its effect to be easily observed, and to estimate its value from Im Z_{HL} and C_e. If the electromagnetic environment around the cell does not change and no shielding is required, C_{hl} values could be comparable to the uncertainty of the impedance analyser. Their effects, however, could still be considerable if electrode capacitance is small because those effects depend on C_{hl}/C_x not just on C_{hl}.

The leakage resistance R_{hl} between electrodes, which can easily decrease well below electrode resistance if the surface of insulators becomes moist, increases Re Z_{HL} for decreasing frequencies and its value largely deviates from R_x. Attempts to determine conductivity from R_x can become frustrated, particularly for high-conductivity samples as these would need to be measured at yet higher frequencies, which are not appropriate because of wave propagation effects.

V. CONCLUSIONS

Interelectrode impedance in a cell intended for water conductivity measurements has been modelled by considering dc leakage resistance in addition to interelectrode capacitance. This capacitance decreases the value of the real part of the measured impedance, which ideally should provide the conductivity value. In addition, it attenuates the real part of the impedance at frequencies below the characteristic frequency of water. Further, it adds to the equivalent series capacitance between the measurement terminals, that otherwise would depend on the material and electrodes. An electric shield around the cell fixes that capacitance but increases its value.

The finite resistance between electrodes is effectively connected in parallel with electrode resistance (that of the insulating container that holds the sample). The effect of those resistances is an increase of the real part of the impedance for decreasing frequencies. To avoid this effect, measurements should be performed at higher frequencies. However, for highly conductive samples such as some water solutions, measurements at those frequencies can be affected by wave propagation effects.

Therefore, high conductivity solutions require excellent insulation in the cell, clean support surfaces between electrodes, and fixed electromagnetic environment with no conductors close to the cell. This is challenging if the cell is connected to a (grounded) impedance analyser.

ACKNOWLEDGEMENT

The authors thank the Castelldefels School of Telecommunication and Aerospace Engineering (EETAC-UPC, BarcelonaTech) for its research facilities and Mr. F. López for his technical support.

REFERENCES

[1] W. Göpel, J. Hesse, and J. N. Zemel, Sensors. A Comprehensive Survey, Vol. 2, Weinheim, Germany: VCH Verlagsgesellschaft mbH, 1991, ch. 7, sec. 3, pp. 314-332.

[2] M. Ballico, "A technique for in situ measurement of the conductivity of water in 'triple point of water' cells," Meas. Sci. Technol., vol. 10, no. 7, pp. L33-L36, July 1999.

[3] M. S. A. Abouelwafa, and E. J. M. Kendall, "The use of capacitance sensors for phase percentage determination in multiphase pipelines," IEEE Trans. Instrum. Meas.,vol. 29, no. 1, pp. 24-27, March 1980.

[4] Reference Data for Radio Engineers, Howard W. Sams & Co., Inc., 6th Ed., New York, International Telephone and Telegraph Corp., 1977, pp.4.28-4.31.

[5] A. Stogryn, "Equations for calculating the dielectric constant of saline water," IEEE Trans. Microwave Tech., vol. MTT-19, pp. 733–736, Aug.1971.

[6] A. Straub, "Boundary element modelling of a capacitive probe for in situ soil moisture characterization," IEEE Trans. Geosci. Remote Sens., vol. 32, no 2, pp. 261-266, Mar. 1994.